



**Retinal is formed from apo-carotenoids in Nostoc sp.  
PCC7120: in vitro characterization of an apo-carotenoid  
oxygenase**

Daniel Scherzinger, Sandra Ruch, Daniel Paul Kloer, Annegret Wilde, Salim Al-Babili

► **To cite this version:**

Daniel Scherzinger, Sandra Ruch, Daniel Paul Kloer, Annegret Wilde, Salim Al-Babili. Retinal is formed from apo-carotenoids in Nostoc sp. PCC7120: in vitro characterization of an apo-carotenoid oxygenase. *Biochemical Journal*, 2006, 398 (3), pp.361-369. 10.1042/BJ20060592 . hal-00478580

**HAL Id: hal-00478580**

**<https://hal.science/hal-00478580>**

Submitted on 30 Apr 2010

**HAL** is a multi-disciplinary open access archive for the deposit and dissemination of scientific research documents, whether they are published or not. The documents may come from teaching and research institutions in France or abroad, or from public or private research centers.

L'archive ouverte pluridisciplinaire **HAL**, est destinée au dépôt et à la diffusion de documents scientifiques de niveau recherche, publiés ou non, émanant des établissements d'enseignement et de recherche français ou étrangers, des laboratoires publics ou privés.

# **Retinal is formed from apo-carotenoids in *Nostoc* sp. PCC7120: *In vitro* characterization of an apo-carotenoid oxygenase**

**Daniel Scherzinger<sup>\*</sup>, Sandra Ruch<sup>\*</sup>, Daniel P. Kloer<sup>†</sup>, Annegret Wilde<sup>‡</sup> and Salim Al-Babili<sup>\*1</sup>**

<sup>\*</sup> Albert-Ludwigs University of Freiburg, Institute of Biology II, Cell Biology, Schaezlestr. 1, D-79104 Freiburg, Germany.

<sup>†</sup> Albert-Ludwigs University of Freiburg, Institute of Organic Chemistry and Biochemistry, Albertstr. 1, D-79104 Freiburg, Germany.

<sup>‡</sup> Humboldt University Berlin, Institute of Biology, Plant Biochemistry, Chausseestr. 117, D-10115 Berlin, Germany.

<sup>1</sup>To whom correspondence should be addressed: Salim Al-Babili, Albert-Ludwigs University of Freiburg, Institute for Biology II, Cellbiology, Schaezlestr. 1, D-79104 Freiburg, Germany.

Tel.: +49 761 203 8454

Fax: +49 761 203 2675

E-mail: [salim.albabili@biologie.uni-freiburg.de](mailto:salim.albabili@biologie.uni-freiburg.de)

## SYNOPSIS

The sensory rhodopsin from *Anabaena (Nostoc)* sp. PCC7120 is the first cyanobacterial retinylidene protein identified. Here, we report on NosACO, encoded by the ORF *all4284*, as the candidate responsible for the formation of the required chromophore, retinal. In contrast to enzymes from animals, NosACO converts  $\beta$ -apo-carotenals instead of  $\beta$ -carotene into retinal *in vitro*. The identity of the enzymatic products was proven by HPLC and GC-MS. NosACO exhibits a wide substrate specificity with respect to chain lengths and functional end-groups converting  $\beta$ -apo-carotenals, (3R)-3-OH- $\beta$ -apo-carotenals and the corresponding alcohols into retinal and 3(R)-3-OH-retinal, respectively. However, kinetic analyses revealed very divergent  $K_m$  and  $V_{max}$  values. Based on the crystal structure of SynACO, a related enzyme from *Synechocystis* sp. PCC6803 showing similar enzymatic activity, we designed a homology model of the native NosACO. The deduced structure explains the absence of  $\beta$ -carotene-cleavage activity and indicates that NosACO is a monotopic membrane protein. Accordingly, NosACO could be readily reconstituted into liposomes. To localize SynACO *in vivo*, a *Synechocystis* knock-out strain was generated expressing SynACO as the sole carotenoid oxygenase. Western blot analyses showed that the main portion of SynACO occurred in a membrane-bound form.

**Key words:** Carotenoid Cleavage, Carotenoid Oxygenase, Cyanobacteria, Opsin, Retinal.

**Abbreviations used:** DTT, dithiothreitol; GC-MS, gas chromatography-mass spectrometry; SynACO, *Synechocystis* apo-carotenoid oxygenase; NosACO, *Nostoc* apo-carotenoid oxygenase.

## INTRODUCTION

Retinal represents the chromophore of the widespread family of retinylidene proteins, commonly called rhodopsins. These light-responsive seven-helix transmembrane proteins are common in archaea, algae and animals. In addition, they have recently been discovered in Eubacteria and Fungi. The basic reaction catalyzed by rhodopsins is the light-dependent *cis-trans* isomerization of retinal, attached in a Schiff base linkage to a lysine residue in the seventh helix, across one of the double bonds in the polyene chain [for review see 1, 2].

Cyanobacteria employ different receptors for sensing light [for review see 3]. It was shown that they contain phytochromes, cryptochromes and, as recently reported, rhodopsin [4]. There have been earlier indications for the occurrence of retinylidene receptors in cyanobacteria like *Calothrix* [5] and *Leptolyngbya* [6] and direct evidence was delivered by Jung *et al.* [4], who identified a sensory rhodopsin from *Anabaena (Nostoc)* sp. PCC7120 (hereafter *Nostoc* sp. PCC7120). The *Anabaena* Sensory Rhodopsin (ASR) has been a subject of comprehensive analyses including its photochemical characteristics and structure at atomic level. ASR shows unique characteristics regarding its interacting transducer, its photocycle and the isomeric state of the bound chromophore upon light and dark adaptation. In addition, it was shown that ASR exhibits light-induced reversible interconversion between 13-*cis* and all-*trans* retinal leading to a wavelength-dependent isomer ratio [4, 7-9]. Therefore, ASR may act as a sensor for light-regulated, color-sensitive processes such as chromatic adaptation [10].

The chromophore of rhodopsins, retinal, is a C<sub>20</sub>-isoprenoid which is usually synthesized as a cleavage product of carotenoids. In animals, retinal is formed through symmetrical oxidative cleavage of  $\beta$ -carotene (C<sub>40</sub>) at the central C15-C15' double bond. The corresponding enzyme 15,15' BCO ( $\beta$ - $\beta$ -Carotene-15,15'-Oxygenase), also named BCO I, is a member of the widespread carotenoid oxygenase family and has been identified from *Drosophila melanogaster* [11], chicken [12] and mammals [13, 14]. Biochemical studies of human BCO I, expressed in insect cells and purified to homogeneity, suggested that at least one unsubstituted  $\beta$ -ionone ring half-site was compulsory for effective cleavage of the carotenoid substrate [15]. It has also been shown that the 15,15' BCO I acts as a monooxygenase [16]. However, recent investigations of AtCCD1 (*A. thaliana* Carotenoid Cleavage Dioxygenase 1) suggested a dioxygenase mechanism [17].

The identification of BCO I has become possible through its sequence homology to Viviparous14 (VP14) from maize, the first carotenoid cleavage enzyme characterized. VP14 represents a non-heme iron oxygenase that catalyzes the oxidative cleavage of 9-*cis*-violaxanthin and 9'-*cis*-neoxanthin, leading to xanthoxin, the precursor of the phytohormone abscisic acid, ABA [18]. This cleavage reaction seems to be key regulatory in the biosynthesis of ABA [19-22]. Database information for sequenced genomes reveals the occurrence of homologous enzymes in all taxa [for review see 23, 24] indicating that VP14 is a member of a widespread oxygenase family involved in

different physiological processes. For instance, the genome of *A. thaliana* encodes 9 putative carotenoid oxygenases [25] catalyzing different cleavage reactions [24]. The cloning of VP14 also led to the identification of carotenoid cleavage enzymes responsible for the synthesis of well known apo-carotenoid pigments, such as bixin in *Bixa orellana* [26] and saffron in *Crocus sativus* [27]. It was also shown that the VP14-homolog, Carotenoid Cleavage Dioxygenase 1 (CCD1), catalyzes the cleavage of several carotenoids leading to the formation of C<sub>13</sub> volatile compounds like  $\beta$ -ionone in *A. thaliana* [28], tomato [29] and petunia flowers [30]. Recent studies revealed that members of the carotenoid oxygenase family are involved in plant development mediating the synthesis of a yet unknown, carotenoid-derived compound, which regulates the apical dominance [31-34].

Recently, we have described an Apo-carotenoid Cleavage Oxygenase (ACO) from *Synechocystis* sp. PCC6803 (SynACO, formerly named Diox1) as the first retinal-forming enzyme of eubacterial origin. In contrast to the related BCO I from animals, SynACO does not utilize  $\beta$ -carotene, but several carotenoid-cleavage products named apo-carotenoids, e.g. 3-OH-apo-carotenoids, to form retinal and retinal-like compounds [35]. As the first member of the widespread carotenoid oxygenase family, the crystal structure of SynACO was recently solved at 2.4 Å resolution, revealing the reaction center geometry and establishing a solid base for modeling of other family members [36].

The occurrence of a functional sensory rhodopsin in *Nostoc* sp. PCC7120 implies the ability of this cyanobacterium to synthesize the chromophore, retinal. The genome of this filamentous cyanobacterium encodes 3 members of the carotenoid oxygenase family (ORFs: *all4284*, *all4895* and *all1106*) which may catalyze retinal-synthesis. Here, we report that the ORF *all4284*-encoded polypeptide (here named NosACO) is an apo-carotenoid cleaving, retinal-forming enzyme showing similar enzymatic activity to SynACO from *Synechocystis* sp. PCC6803. In addition, reconstitution of NosACO and localization of SynACO indicated that both polypeptides are membrane-bound. The obtained experimental data were corroborated by a model of NosACO deduced from the crystal structure of SynACO. Our data indicate that the cleavage of apo-carotenoids to form retinal and retinal-like compounds is probably a widespread reaction in cyanobacteria.

## EXPERIMENTAL

### Cultures of cyanobacteria

*Nostoc* sp. PCC7120 cells were cultured in liquid BG11<sub>0</sub> medium [37] supplemented with 10 mM NaHCO<sub>3</sub>. The *Synechocystis* sp. PCC6803 *SynDiox2* knock-out strain was grown in BG11 medium [37] containing 15 µg/ml chloramphenicol. Cultures were grown in Erlenmeyer flasks under constant illumination of 15 µmol photons/m<sup>2</sup>·s at 30 °C.

### Cloning of *Nostoc* carotenoid oxygenases

The gene *all4284* coding for NosACO (accession number: NP\_488324) was amplified using the primer pair NosACO-for: 5'-ATGCAAAGTTACAAATATCAACA-3' and NosACO-back: 5'-TTATACAAATACCTGGGGAGTAA-3'. The ORFs *all4895* and *all1106*, encoding the other two carotenoid oxygenases from *Nostoc*, were amplified using the primer pairs ND2F/ND2B (5'-ATGCAGATAGTTGATAAAAGGTCA-3'; 5'-TTATCTCTTCTCTGATTTCATGT-3') and ND3F/ND3B (5'-ATGGTAAAAGATTCACTCACTTTC-3'; 5'-TTAAATTCTCCTAAAATTCAACTGTTC-3'), respectively. The PCR reactions were carried out using about 100 ng genomic DNA, 100 ng of each primer, 200  $\mu$ M dNTPs and 1  $\mu$ l Advantage<sup>®</sup> cDNA Polymerase Mix (BD Biosciences, CA, USA) in the buffer provided, as follows: 2 min initial denaturation at 94 °C followed by 32 cycles (30 s 94 °C, 30 s 56 °C, 2 min 68 °C) and 10 min final polymerization at 68 °C. The obtained PCR products were purified using GFX<sup>™</sup> PCR DNA and Gel Band Purification Kit (Amersham Biosciences, NJ, USA), and cloned into the pCR2.1<sup>®</sup>-TOPO<sup>®</sup> and pBAD/TOPO<sup>®</sup>-ThioFusion<sup>™</sup> vectors (Invitrogen, Paisley, UK). The nature of the products was verified by sequencing. The obtained pBAD/TOPO<sup>®</sup>-ThioFusion<sup>™</sup> vectors were used for the expression in carotenoid-accumulating *E. coli* cells. The vectors pNosACO-CR2.1, pND2-CR2.1 and pND3-CR2.1 which carry *NosACO*, *NosDiox2* and *NosDiox3* were used for further cloning.

### Protein expression and purification

NosACO was expressed as a glutathione-S-transferase (GST) fusion protein. For this purpose, *NosACO* was excised from pNosACO-CR2.1 using *Eco*RI, and ligated into *Eco*RI/CIP treated pGEX-5X-1 (Amersham Biosciences, NJ, USA) to yield the vector pGEX-5X-NosACO. Subsequently, *BL21* *E. coli* cells were transformed with pGEX-5X-NosACO, grown at 37 °C in 2X YT-medium and induced at an OD<sub>600</sub> of 0.5 with 0.2 mM IPTG. After incubation for additional 4 h at 28 °C, cells were harvested by centrifugation, resuspended in phosphate-buffered saline (PBS) and lysed in a French press. The fusion protein was then purified using glutathione-sepharose 4B (Amersham Biosciences, NJ, USA), and NosACO was released by overnight treatment with the protease factor X<sub>a</sub> in PBS containing 0.1% (v/v) Triton X-100 at room temperature, according to the instructions of the manufacturer (Amersham Biosciences, NJ, USA). For the reconstitution assays, NosACO was released in PBS containing 1% (w/v) octyl- $\beta$ -glucoside. Purification steps and protein expression were analyzed by SDS-PAGE.

### Analyses of the membrane association

All steps were performed in 100 mM Bistris/HCl, pH 6.8, buffer containing 1 mM DTT. For preparation of liposomes 1,2-diacyl-sn-glycero-3-phosphocholine from soybean (Sigma, Deisenhofen, Germany) was solubilized in chloroform/MeOH (2:1, v/v),  $\beta$ -apo-8'-carotenal was then added to a final concentration of 30  $\mu$ M. After drying, the buffer was added to obtain a final lipid concentration

of 1 mg/ml. After incubation for 1 h on ice, liposomes were obtained by sonication on ice. 720  $\mu$ l purified NosACO (about 1.2  $\mu$ g/ $\mu$ l) in PBS containing 1% (w/v) octyl- $\beta$ -glucoside was diluted (1:5) with the liposomes and incubated on ice for 10 min. Liposomes were pelleted at 100.000 g for 30 min, washed with 3.6 ml buffer, pelleted again and resuspended in the same volume of the buffer.

For the salt-treatment, 1.8 ml liposomes suspension, containing NosACO and prepared as described above, was adjusted to a final concentration of 0.2 M KCl and incubated on ice for 10 min. Liposomes were then harvested by centrifugation at 100.000 g for 30 min, washed in 1.8 ml buffer, pelleted again and resuspended in 1.8 ml buffer.

Samples corresponding to equal portions of each fraction were subjected to SDS-PAGE and analyzed by western blotting using the ECL<sup>TM</sup> Western Blotting Analysis System (Amersham Biosciences, NJ, USA). NosACO was detected using mice polyclonal anti-SynACO-antibodies raised against overexpressed and purified enzyme [36].

*Synechocystis SynDiox2 knock-out* cultures were harvested, washed and resuspended in PBS. The cells were broken by four passages through a French press cell at 18.000 psi. Cell debris was removed by repeated centrifugation for 10 min at 4.000 g. The obtained supernatant was then separated into a membrane and a cytoplasmic fraction by centrifugation for 4 h at 130.000 g. Membranes were washed with PBS, pelleted by centrifugation at 130.000 g for 2 h and resuspended in PBS. Samples containing equal protein amounts from each fraction were analyzed by SDS-PAGE and western blotting using the ECL<sup>TM</sup> Western Blotting Analysis System (Amersham Biosciences, NJ, USA) and mice polyclonal anti-SynACO-antibodies.

### Enzyme assays

Substrates were purified according to [35]. Synthetic apo-carotenals were kindly provided by BASF (Ludwigshafen, Germany). The corresponding alcohols were obtained by reduction of the aldehydes with NaBH<sub>4</sub> in EtOH. Enzyme assays were performed according to [26] with some modifications. Substrates were mixed with an EtOH solution of octyl- $\beta$ -glucoside, dried using a vacuum centrifuge and then resuspended in water. The final concentration of the apo-carotenoid substrates was 40  $\mu$ M, the concentration of octyl- $\beta$ -glucoside 1% (w/v). The incubation buffer contained 1 mM DTT and 1 mg/ml catalase (Sigma, Deisenhofen, Germany) in 200  $\mu$ l of 100 mM Bistris/HCl, pH 6.8. Purified NosACO was then added to obtain a concentration of 100 ng/ $\mu$ l. Assays were incubated at 27 °C for 2 h. For GC-MS identification of the cleavage products the assay volume was 2 ml with incubation for 2.5 h. The assays were stopped by adding one volume of acetone and extracted using petroleum benzene/diethylether (1:4, v/v). The analysis was carried out as given below.

### Analytical methods

Substrates and products were quantified spectrophotometrically at their individual  $\lambda_{\text{max}}$  using extinction coefficients calculated from E1% as given by Barua and Olson [37] or as determined with

the synthetic compounds (BASF, Ludwigshafen, Germany). Protein concentration was determined using the BioRad protein assay kit (BioRad, CA, USA). For HPLC, a Waters system (Eschborn, Germany) equipped with a photodiode array detector (model 996) was used. The separation was performed using a C<sub>30</sub>-reversed phase column (YMC Europe, Schermbeck, Germany) with the solvent systems B: MeOH/*tert*-butylmethyl ether/water (120:4:40, v/v/v) and A: MeOH/*tert*-butylmethyl ether (500:500, v/v). The column was developed at a flow-rate of 1 ml/min with a gradient from 100% B to 43% B within 45 min, then to 0% B within 1 min, maintaining the final conditions for another 14 min at a flow-rate of 2 ml/min.

### GC-MS analyses

To remove detergents present in the extracts, products were pre-purified by TLC using RP-18 F<sub>245s</sub> plates (Merck, Darmstadt, Germany). All plates were washed in a chromatographic step with chloroform prior to use. The plates were developed in MeOH/water (100:1, v/v). Products were then scraped off and eluted with chloroform, evaporated and redissolved in acetone for analyses. GC-MS analyses were performed according to [35] using a Finnigan Trace DSQ mass spectrometer coupled to a Trace GC gas chromatograph. Identification of compounds was done by chromatographic comparison with the authentic references and by comparing the mass spectra with the NIST Mass Spectral Search Program Version 2.0 (National Institute of Standards and Technology).

### Kinetic analyses

Measurements were carried out photometrically at 20 °C using a UV-2501PC spectrophotometer (Shimadzu, Japan). The assays contained 100 mM Bistris/HCl, pH 6.8, 1% (w/v) octyl- $\beta$ -glucoside, 1 mM DTT, 200 ng/ml catalase and purified NosACO at a concentration of 30 ng/ $\mu$ l in a final volume of 700  $\mu$ l. The concentrations of the apo-carotenoid substrates used ranged from 5 to 80  $\mu$ M. The formation of the C<sub>20</sub> cleavage products was determined during an incubation of 5 to 15 min. Time intervals with maximum velocity were used for further calculations. The enzyme kinetics were calculated using the solver function of MS-Excel. This function fits the data to the Michaelis-Menten equation using non-linear regression analysis.

### Homology modeling

A homology model of NosACO was built using the published coordinates of SynACO (PDB code 2BIX) as template. Model building and energy minimization was performed using SWISS-MODEL [38] in first approach mode. Solvent-accessible surfaces were generated with MSMS [39] and analyzed with PISA [40].



### Generation of the *Synechocystis* *SynDiox2* knock-out strain

A 557-bp fragment (*delta5*), representing a stretch of the 5'-non-coding region and a part of *SynDiox2*, and a 448-bp fragment (*delta3*), corresponding to the 3'-non-coding region and a part of *SynDiox2*, were amplified from 25 ng *Synechocystis* sp. PCC6803 genomic DNA using Advantage<sup>®</sup> cDNA Polymerase Mix (BD Biosciences, CA, USA) in the buffer provided. The PCR reactions were performed using the primer pair I/II and III/IV for the amplification of *delta5* and *delta3*, respectively (I: 5'-GGGCCGCTACTCGAGCCAGTCTG-3'; II: 5'-TCCTCTGCGTAAGCTTGGGTTTGC-3'; III: 5'-ACCGGCGGAATTCCTTGGTTC-3'; IV: 5'-TGCTTAATGAGCTCTCCAGTTTCA-3'). Both fragments were then cloned sequentially into pKSCm2, a pBluescript KS with a *cat* (chloramphenicol transferase) gene cassette integrated into the *EcoRV* site, after *XhoI/HindIII* (for *delta5*) and *EcoRI/XbaI* (for *delta3*) digestion. The correctness of the resulting suicide vector pDiox2Knock was proofed by DNA sequencing. pDiox2Knock, bearing a chloramphenicol resistance cassette between *delta5* and *delta3* in antisense orientation, was then transformed into wild-type cells of *Synechocystis* sp. PCC6803 according to Ermakova *et al.* [41]. The absence of the wild-type allele in fully segregated mutants was verified by PCR using the primers Co1: 5'-AGTTTGTGACCCAGACCGATGTA-3' and Co2: 5'-ATAGTTGACCATCCGTGGAGGTTT-3'.

## RESULTS

### $\beta$ -carotene is not cleaved by any of the three *Nostoc* carotenoid oxygenases

To determine the enzyme catalyzing the formation of retinal, the three *Nostoc* ORFs *all4284* (here *NosACO*), *all4895* (*NosDiox2*) and *all1106* (*NosDiox3*) encoding putative carotenoid oxygenases were cloned and expressed in  $\beta$ -carotene accumulating *E. coli* cells. However, none of the expressed enzymes was capable of converting  $\beta$ -carotene as determined by the absence of cleavage products in HPLC analyses (data not shown).

### *NosACO* converts apo-carotenals into retinal

Since no cleavage activity was observed in carotenoid-accumulating *E. coli* cells, *in vitro* assays were performed using total lysate of cells expressing *NosACO*, *NosDiox2* and *NosDiox3*, respectively. Subsequent analyses revealed that none of the expressed oxygenases is capable of  $\beta$ -carotene cleavage. Therefore, apo-carotenals with different chain lengths were applied. Subsequent HPLC analyses showed that *NosACO* converted apo-carotenoids with different chain lengths into a compound resembling retinal (C<sub>20</sub>), while the products obtained from *NosDiox2* and *NosDiox3* were different in chain lengths depending on the substrates applied (data not shown). This indicated that *NosACO* is the candidate for retinal formation. For a more comprehensive investigation of its enzymatic activity, *NosACO* was expressed as a GST fusion, purified using glutathione-sepharose and released by the protease factor X<sub>a</sub> (supplemental Fig. 1). Here again, *in vitro* assays using the

purified enzyme and major carotenoid compounds of *Nostoc*, e.g.  $\beta$ -carotene, echinenone and myxoxanthophyll, did not show any cleavage activity, while apo-carotenals were converted readily. As can be seen in Fig. 1, a striking activity was observed with  $\beta$ -apo-8'-carotenal which was converted by NosACO into a compound that resembled retinal in its UV/Vis spectrum and its chromatographic behavior on HPLC. To prove its identity, GC-MS analyses were carried out using retinal as a standard, which showed an identical retention time. The mass spectrum obtained was identical with published data [35, 43] and with spectra in the NIST database, including the presence of the correct molecular ion of  $m/z = 284$  (Fig. 2). Thus, NosACO converted the  $C_{30}$  substrate into retinal ( $C_{20}$ ). The catalytic activity of NosACO should also lead to a second product(s) with a chain length of  $C_{10}$  or shorter. Indeed, apo-8',15'-apo-carotene-dial (2,6-dimethyl-octa-2,4,6-trien-dial,  $C_{10}O_2H_{11}$ ) was detected and proven by HPLC (Fig. 1) and GC-MS analyses (Fig. 2) as a second product showing the chromatographic characteristics and the EI mass spectrum of the authentic reference compound (kindly provided by BASF, Ludwigshafen, Germany). Taken together, the nature of the products identified demonstrates the cleavage of the used apo-carotenoids at the  $C_{15}$ - $C_{15'}$  double bond (Fig. 3).

### Substrate specificity of NosACO

The *Synechocystis* enzyme SynACO was shown to cleave a wide range of different apo-carotenoids [35]. To investigate the end-group specificity of NosACO, (3R)-3-OH- $\beta$ -apo-8'-carotenal formally derived from zeaxanthin was used *in vitro* as described. As shown by HPLC analysis (Fig. 1), this substrate was converted by the enzyme into (3R)-3-OH-retinal and apo-8',15'-apo-carotene-dial. The nature of the  $C_{20}$ -product obtained was further confirmed by GC-MS-analysis (Fig. 2) revealing a correct molecular ion of  $m/z = 300$  and a mass spectrum identical to that of the authentic reference compound (kindly provided by BASF, Ludwigshafen, Germany). Further, we tested  $\beta$ -apo-8'-carotenol and the corresponding alcohols of the above mentioned substrates. Here again, retinal or the corresponding  $C_{20}$  compounds were produced. To determine the chain length specificity, we performed *in vitro* assays with  $\beta$ -apo-4'-carotenal ( $C_{35}$ ),  $\beta$ -apo-10'-carotenal ( $C_{27}$ ),  $\beta$ -apo-12'-carotenal ( $C_{25}$ ) and (3R)-3-OH- $\beta$ -apo-12'-carotenal. The subsequent analysis showed that NosACO cleaved  $\beta$ -apo-10'-carotenal and (3R)-3-OH- $\beta$ -apo-12'-carotenal forming retinal and (3R)-3-OH-retinal, respectively (data not shown). In addition, the enzyme also cleaved apo-10'-lycopenal into acycloretinal (data not shown). In contrast,  $\beta$ -apo-12'-carotenal ( $C_{25}$ ) and  $\beta$ -apo-4'-carotenal ( $C_{35}$ ) were not cleaved. The substrates and the corresponding chemical structures are given in Fig. 3.

### Kinetic analyses

The data given above suggest a wide substrate specificity. However, the cleavage reactions exhibited very divergent initial reaction velocities depending on the substrate employed. For instance, apo-8'-lycopenal was converted obviously at a slow rate as compared to  $\beta$ -apo-8'-carotenal. Kinetic

analyses were performed with the substrates  $\beta$ -apo-8'-carotenal,  $\beta$ -apo-10'-carotenal,  $\beta$ -apo-8'-carotenol and (3R)-3-OH- $\beta$ -apo-8'-carotenal exhibiting different chain lengths and functional groups. Table 1 gives the  $K_m$  and  $V_{max}$  values determined in the biphasic detergent-containing *in vitro* incubation system used. The lowest  $K_m$  values were obtained for (3R)-3-OH- $\beta$ -apo-8'-carotenal, followed by  $\beta$ -apo-8'-carotenal,  $\beta$ -apo-10'-carotenal and finally by  $\beta$ -apo-8'-carotenol. However,  $\beta$ -apo-8'-carotenal showed lower  $V_{max}$  values when compared to the corresponding alcohol, i.e., NosACO exhibited a higher affinity to aldehydes but converted alcohols faster. In addition,  $\beta$ -apo-8'-carotenal showed also a significantly higher  $V_{max}$  than (3R)-3-OH- $\beta$ -apo-8'-carotenal indicating that the enzyme converted unsubstituted substrates faster than (3R)-3-OH- $\beta$ -derivatives. Although, the determined  $K_m$  values for  $\beta$ -apo-8'-carotenal ( $C_{30}$ ) and  $\beta$ -apo-10'-carotenal ( $C_{27}$ ) were similar, the  $C_{30}$ -substrate was converted much faster, as indicated by the  $V_{max}$  values.

### Structure alignment with SynACO and modeling

The observed enzymatic activity of NosACO resembles the one described for SynACO from *Synechocystis* [35]. In addition, both enzymes belong to the same family and share about 53% identity at amino acid level. The recently solved crystal structure of SynACO [36] allowed the construction of a homology model of NosACO. In the structure-based sequence alignment used, there are no gaps within secondary structure elements (supplemental Fig. 2). Two small insertions of two residues each occur in NosACO as compared to SynACO. Both are located in a loop between  $\beta$ -strands 18 and 19 and were modeled with good stereochemistry. All other residues of the NosACO sequence were exactly superimposable onto the template. Given the high degree of sequence identity between SynACO and NosACO, the resulting homology model is expected to be exact within a 1.5 Å root mean square deviation with respect to  $C_\alpha$  positions [44]. All residues known to be important for substrate binding and catalysis in SynACO are found at corresponding positions in the NosACO homology model. NosACO consists of a single domain and adopts a  $\beta$ -propeller fold with seven propeller blades (Fig. 4). Long loops on the top side of the  $\beta$ -propeller form a dome covering the active site, which is located in the center of the protein at the propeller axis. The catalytic center is formed by four histidine residues that are strictly conserved in all carotenoid cleavage oxygenases and coordinates a ferrous iron ion. Interestingly, all residues lining the hydrophobic substrate tunnel in SynACO, up to 10 Å away from the catalytic center, are either identical or conservatively replaced by residues with the same steric requirements in NosACO, giving rise to a substrate binding cavity with an almost identical shape (Fig. 4). Assuming the same substrate binding geometry as was previously observed in SynACO [36], the homology model clearly predicts that  $C_{40}$  substrates will not be cleaved by NosACO. On the surface of NosACO, a large nonpolar patch consisting of leucine, tryptophane, phenylalanine and isoleucine residues lies at the same position as in SynACO (Fig. 4), while the remaining surface of the molecule is predominantly polar. It was presumed that the corresponding region in SynACO dips into the membrane in order to provide access to the unpolar substrate. The

hydrophobic patch in NosACO is even larger ( $889 \text{ \AA}^2$  as compared to  $800 \text{ \AA}^2$  in SynACO), leading to the prediction that NosACO may also be a monotopic membrane protein.

### NosACO and SynACO are membrane proteins

The lipophilic nature of the substrates as well as the predicted model indicate that NosACO is a membrane protein. Therefore, we performed reconstitution assays into artificial membranes using the purified enzyme. NosACO could be readily reconstituted as shown in the Western blot analysis (Fig. 5). Additionally, the membrane binding was stable upon high-salt treatment. These data coincide with the structural model and indicate that NosACO is a membrane-bound enzyme.

The genome of *Nostoc* encodes three members of the carotenoid oxygenase family which may not be distinguished by polyclonal antibodies. In contrast, *Synechocystis* contains only two members of this family (SynACO and ORF: *slr648*, hereafter *SynDiox2*). To localize SynACO *in vivo*, we generated a knock-out strain by interrupting *SynDiox2*. Thus, this strain encodes only SynACO and allows, therefore, the localization of SynACO by using polyclonal, anti-SynACO-antibodies avoiding cross-reactions. As can be seen in Fig. 6, only traces of SynACO could be detected in the cytoplasmic fraction, while the main portion of the enzyme occurred in a membrane-bound form.

### DISCUSSION

The *Nostoc* sensory rhodopsin was the first of its kind found in cyanobacteria. Its occurrence implies the biosynthetic capacity for the chromophore, retinal. According to the current state of knowledge, retinal is formed either by a member of the widespread carotenoid-oxygenase family (for review see: 45, 46] or by the very recently described enzyme Blh from marine proteobacteria [47] and its formerly identified halobacterial homologs [48]. Searching the genome of *Nostoc* for putative carotenoid oxygenases revealed the occurrence of three members of this protein family, ORFs: *all4284*, *all4895* and *all1106*, while no sequence with significant similarity to *Blh* was found. This led us to suggest that retinal is formed through one of the encoded carotenoid oxygenases. However, *in vivo* and *in vitro* studies showed that none of these three enzymes is capable of cleaving  $\beta$ -carotene to yield retinal (data not shown) excluding a central cleavage mechanism of  $\beta$ -carotene, as commonly found in animals. Based on our recent finding that the *Synechocystis*-enzyme SynACO forms retinal and retinal-like compounds from apo-carotenoids and not from  $\beta$ -carotene [35], we assumed that *Nostoc* may utilize similar substrates for retinal-formation. Accordingly, we performed *in vitro*-enzymatic analyses using apo-carotenoids as substrates. Among the three carotenoid oxygenases, NosACO, encoded by the ORF *all4284*, was the one to form retinal and derivatives from apo-carotenals with different chain lengths indicating its involvement in retinal supply. Albeit the significance of the sequence homology between SynACO and NosACO (53% identity), it could not necessarily be expected that both enzymes exhibit the same activity and, thus, that both cyanobacteria utilize apo-

carotenals to form retinal. Generally, orthologous carotenoid oxygenases show more pronounced homology. For instance, the carotenoid cleavage dioxygenases 1 (CCD1) from *A. thaliana* [28] and *L. esculentum* [29] share about 79% identity at amino acid level. The sequence divergence between SynACO and NosACO could be explained by the evolutionary distance between the unicellular *Synechocystis* sp. PCC6803 and the axenic, nitrogen fixing *Nostoc* sp. PCC7120.

To characterize the substrate specificity, *in vitro* studies were performed using the purified enzyme. NosACO cleaved  $\beta$ -apo-carotenals with different chain lengths, (3R)-OH- $\beta$ -apo-carotenals as well as the corresponding alcohols. Depending on the nature of the end-groups, the cleavage led to the formation of retinal and (3R)-3-OH-retinal. However, the values determined for  $K_m$  and  $V_{max}$  differed markedly (Table 1). Given that low substrate concentrations prevail *in vivo*, one would assume the preferred natural substrate to be a C3-hydroxylated apo-carotenal with a  $C_{27}$  or  $C_{30}$  chain length. However, the identity of the natural substrate and the reaction leading to its formation are still to be elucidated. Like in *Synechocystis* [35], HPLC analyses of carotenoid extracts from *Nostoc* revealed the occurrence of small amounts of compounds which resembled (3R)-3-OH- $\beta$ -apo-carotenals in their UV/Vis spectra as well as in their elution characteristics (data not shown), but these were too low in abundance to allow an investigation of their molecular structure. Such precursor molecules may be formed through the action of a different enzyme. The two additional members of the carotenoid oxygenase family found in the genome of *Nostoc* are good candidates. Although, our preliminary analyses indicate that none of these enzymes cleaves  $\beta$ -carotene, it cannot be excluded that a (3R)-3-OH-substrate may be supplied by one of these oxygenases through an initial cleavage of myxoxanthophylls which are common in *Nostoc* [49]. However, carotenoids may be also cleaved by enzymes, like peroxidases and lipoxygenases, which do not belong to the carotenoid oxygenase family. For instance, Zorn *et al.* [50] reported on a fungal peroxidase from *Lepista irina* which cleaved  $\beta$ -carotene to form certain flavor compounds. In addition, the genome of *Nostoc* encodes a putative lipoxygenase (ORF *all8020*) with unknown function. Alternatively, apo-carotenoids may arise from photo-destruction processes mediated by reactive oxygen species (ROS), increased under light or salt stress. It was reported that the transcript level of the homologous enzyme SynACO from *Synechocystis* was increased by 4 fold within 15 min after exposure to high light [51] and by 21 fold within 30 min after treatment with 684 mM NaCl [52]. Considering the similarity in the catalytic activity and the amino acid sequence, it appears conceivable that NosACO may be subjected to a similar regulation. In this case, NosACO may convert a non-enzymatically originated, inhomogeneous population of apo-carotenoids into homogeneous  $C_{20}$  compounds, namely retinal, retinol and its in-ring hydroxylated derivatives.

The enzymatic activity of NosACO, the substrate specificity for apo-carotenoids, and the kinetic characteristics resemble those of SynACO [35]. However, NosACO showed more specificity with respect to the substrate's chain lengths and did not convert  $\beta$ -apo-4'- and  $\beta$ -apo-12'-carotenal, which were both cleaved by SynACO [35].

The crystal structure of the latter enzyme allowed to explain and thus supported the experimentally shown absence of  $\beta$ -carotene cleaving activity [35]. SynACO exhibits a substrate cavity with a bottleneck at the entrance arresting the  $\beta$ -ionone ring, thus placing the substrate into the correct position for retinal formation. In other words, the substrate enters the cavity with its open-chain end (Fig. 4), since the  $\beta$ -ionone ring cannot pass. The NosACO model deduced from the structure-based alignment with SynACO showed a very similar geometry of the substrate cavity explaining the observed absence of  $\beta$ -carotene cleaving activity.

Consistent with the lipophilic nature of substrates and products, a further prediction drawn from the NosACO-model is the attribute of being a monotopic membrane protein. In the model, the surface of NosACO exhibits a large nonpolar patch consisting of leucine, tryptophane, phenylalanine and isoleucine residues at the same position as in SynACO. It was presumed that the corresponding region in SynACO dips into the membrane. The reconstitution experiments and localization studies shown here indicate that both enzymes are membrane proteins. In both experiments, only traces of soluble enzymes were detected. Similarly, the xanthoxin-forming enzyme P<sub>v</sub>NCED (*Phaseolus vulgaris* nine-*cis*-epoxy-carotenoid dioxygenase) was found only in the thylakoid fraction of bean leaves [19]. In contrast, it was shown that only about 35% of VP14 from maize are associated with the thylakoid membrane upon import. In addition, Western blot analyses of maize chloroplasts revealed a stromal and a membrane-bound VP14-fraction [25]. It has been speculated that the degree of membrane association may be regulated in intact chloroplasts and that the soluble fraction is inactive [25], as reported for the phytoene desaturase from *Narcissus pseudonarcissus* [53]. The membrane association of VP14 is mediated by an N-terminal amphipathic helix [25]. A more complicated pattern was reported for RPE65 (Retinal Pigment Epithelium 65), an animal member of the carotenoid oxygenase family involved in the visual cycle. RPE65 occurs in a triply palmitoylated, membrane-associated (mRPE65) and in a soluble, un-palmitoylated form (sRPE65). It appears that the palmitoylation determines whether RPE65 binds all-*trans*-retinyl ester (mRPE65) or all-*trans* retinol (sRPE65), and thus, controls the ligand binding selectivity [54]. Taken together, it might be speculated that the soluble traces of SynACO may represent an inactive form.

The model also indicates that the product formed is deposited into membranes through a tunnel and not passed to a cytoplasmic protein. To test this prediction, we conducted *in vitro* assays using artificial membranes containing reconstituted NosACO. The subsequent analyses revealed a clear retinal formation (data not shown). However, the amount of the product was low, compared to the amounts obtained from the detergent-based assays and, therefore, did not allow a clear conclusion about the destination of retinal.

## ACKNOWLEDGEMENTS

This work was supported by the Deutsche Forschungsgemeinschaft (DFG) Grant AL892-1 and by the HarvestPlus programme ([www.harvestplus.org](http://www.harvestplus.org)). We are indebted to Dr. Peter Beyer for valuable discussions. We thank Dr. Hansgeorg Ernst for providing the apo-carotenoids and Dr. Andreas Seidler for his help in constructing the knock-out plasmids.

## REFERENCES

- 1 Spudich, J. L., Yang, C. S., Jung, K. H. and Spudich, E. N. (2000) Retinylidene proteins: structures and functions from archaea to humans. *Annu. Rev. Cell Dev. Biol.* **16**, 365-392
- 2 Zhai, Y., Heijne, W. H. M., Smith, D. W. and Saier, M. H., Jr. (2001) Homologues of archaeal rhodopsins in plants, animals and fungi: structural and functional predictions for a putative fungal chaperone protein. *Biochim. Biophys. Acta* **1511**, 206-223
- 3 Mullineaux, C. W. (2001) How do cyanobacteria sense and respond to light? *Mol. Microbiol.* **41**, 965-971
- 4 Jung, K. H., Trivedi, V. D. and Spudich, J. L. (2003) Demonstration of a sensory rhodopsin in Eubacteria. *Mol. Microbiol.* **47**, 1513-22
- 5 Hoff, W. D., Matthijs, H. C. P., Schubert, H., Crielaard, W. and Hellingwerf, K. J. (1995) Rhodopsin(s) in eubacteria. *Biophys. Chem.* **56**, 193-199
- 6 Albertano, P., Barsant, L., Passarelli, V. and Gaultieri, P. (2000) A complex photoreceptive structure in the cyanobacterium *Leptolyngbya* sp. *Micron* **31**, 27-34
- 7 Sineshchekov, O. A. and Spudich J. L. (2004) Light-induced intramolecular charge movements in microbial rhodopsins in intact *E. coli* cells. *Photochem. Photobiol. Sci.* **3**, 548-554
- 8 Sineshchekov, O. A., Trivedi, V. D., Sasaki, J. and Spudich J. L. (2005) Photochromicity of *Anabaena* sensory rhodopsin, an atypical microbial receptor with *cis*-retinal light adapted form. *J. Biol. Chem.* **15**, 14663-14668
- 9 Vogeley, I., Sineshchekov, O. A., Trivedi, V. D., Sasaki, J., Spudich, J. L. and Lueke, H. (2004) *Anabaena* Sensory Rhodopsin: A photochromic Color Sensor at 2.0 Å. *Science* **306**, 1390-1393
- 10 Grossman, A. R., Bhaya, D. and He, Q. (2001) Tracking the light environment by cyanobacteria and the dynamic nature of light-harvesting. *J. Biol. Chem.* **276**, 11449-11542
- 11 von Lintig, J. and Vogt, K. (2000) Filling the gap in vitamin A research. *J. Biol. Chem.* **275**, 11915-11920
- 12 Wyss, A., Wirtz, G., Woggon, W., Brugger, R., Wyss, M., Friedlein, A., Bachmann, H. and Hunziker, W. (2000) Cloning and expression of beta,beta-carotene 15,15'-dioxygenase. *Biochem. Biophys. Res. Commun.* **271**, 334-336
- 13 Redmond, T. M., Gentleman, S., Duncan, T., Yu, S., Wiggert, B., Gantt, E. and Cunningham, F. X., Jr. (2001) Expression, and Substrate Specificity of a Mammalian  $\beta$ -Carotene 15,15'-Dioxygenase. *J. Biol. Chem.* **276**, 6560-6565
- 14 Yan, W., Jang, G. F., Haeseleer, F., Esumi, N., Chang, J., Kerrigan, M., Campochiaro, M., Campochiaro, P., Palczewski, K. and Zack, D. J. (2001) Cloning and characterization of a human beta,beta-carotene-15,15'-dioxygenase that is highly expressed in the retinal pigment epithelium. *Genomics* **72**, 193-202



- 15 Lindqvist, A. and Andersson, S. (2002) Biochemical properties of purified recombinant human beta-carotene 15,15'-monooxygenase. *J. Biol. Chem.* **277**, 23942-23948
- 16 Leuenberger, M. G., Engeloch-Jarret, C. and Woggon, W. (2001) The reaction mechanism of the enzyme catalyzed central cleavage of  $\beta$ -carotene to retinal. *Angew. Chem.* **113**, 2684-2687
- 17 Schmidt, H., Kurtzer, R., Eisenreich, W. and Schwab, W. (2006) The carotenase AtCCD1 from *Arabidopsis thaliana* is a Dioxygenase. *J. Biol. Chem.* **281**, 9845-9851
- 18 Schwartz, S. H., Tan, B. C., Gage, D. A., Zeevart, J. A., and McCarty D. R. (1997) Specific Oxidative Cleavage of Carotenoids by VP14 of Maize. *Science* **276**, 1872-1874
- 19 Qin, X. and Zeevaart, J. A. (1999) The 9-*cis*-epoxycarotenoid cleavage reaction is the key regulatory step of abscisic acid biosynthesis in water-stressed bean. *Proc. Natl. Acad. Sci. USA* **96**, 15354-15361
- 20 Thompson, A. J., Jackson, A. C., Symonds, R. C., Mulholland, B. J., Dadswell, A. R., Blake, P. S., Burbidge, A. and Taylor, I. B. (2000) Ectopic expression of a tomato 9-*cis*-epoxycarotenoid dioxygenase gene causes over-production of abscisic acid. *Plant J.* **23**, 363-274
- 21 Iuchi, S., Kobayashi, M., Taji, T., Naramoto, M., Seki, M., Kato, T., Tabata, S., Kakubari, Y., Yamaguchi-Shinozaki, K. and Shinozaki K. (2001) Regulation of drought tolerance by gene manipulation of 9-*cis*-epoxycarotenoids dioxygenase, a key enzyme in abscisic acid biosynthesis in *Arabidopsis*. *Plant J.* **27**, 325-333
- 22 Qin, X. and Zeevaart, J. A. (2002) Overexpression of a 9-*cis*-epoxycarotenoid dioxygenase gene in *Nicotiana glauca* increases abscisic acid and phaseic acid levels and enhances drought tolerance. *Plant Physiol.* **128**, 544-551
- 23 Guiliano, G., Al-Babili, S. and von Lintig, J. (2003) Carotenoid oxygenases: cleave it or leave it. *Trends Plant Sci.* **8**, 145-149
- 24 Camara, B. and Bouvier, F. (2004) Oxidative remodeling of plastid carotenoids. *Arch. Biochem. Biophys.* **430**, 16-21
- 25 Tan, B. C., Joseph, L. M., Deng, W. T., Liu, L., Li, Q. B., Cline, K. and McCarty, D. R. (2003) Molecular characterization of the *Arabidopsis* 9-*cis* epoxycarotenoid dioxygenase gene family. *Plant J.* **35**, 44-56
- 26 Bouvier, F., Suire, C., Mutterer J. and Camara, B. (2003) Oxidative remodeling of chromoplast carotenoids: Identification of the carotenoid dioxygenase *CsCCD* and *CsZCD* genes involved in Crocus secondary metabolite biogenesis. *Plant Cell* **15**, 47-62
- 27 Bouvier, F., Dogbo, O. and Camara, B. (2003) Biosynthesis of the food and cosmetic plant pigment bixin (annatto). *Science* **300**, 2089-2091
- 28 Schwartz, S. H., Xiaoqiong, Q. and Zeevart, J. A. (2001) Characterization of a Novel Carotenoid Cleavage Dioxygenase from Plants. *J. Biol. Chem.* **276**, 25208-25211

- 29 Simkin, A. J., Schwartz, S. H., Auldrige, M., Taylor, M. G. and Klee, H. J. (2004) The tomato *carotenoid cleavage dioxygenase 1* genes contribute to the formation of the flavor volatiles  $\beta$ -ionone, pseudoionone, and geranylacetone. *Plant J.* **40**, 882-892
- 30 Simkin, A. J., Underwood, B. A., Auldrige, M., Loucas, H. M., Shibuya, K., Schmelz, E., Clark, D. G. and Klee, H. J. (2004) Circadian regulation of the PhCCD1 carotenoid cleavage dioxygenase controls emission of beta-ionone, a fragrance volatile of petunia flowers. *Plant Physiol.* **136**, 3504-3514
- 31 Ward, S. P. and Leyser, O. (2004) Shoot branching. *Curr. Opin. Plant Biol.* **7**, 73-78
- 32 Schwartz, S. H., Qin, X. and Loewen, M. C. (2004) The biochemical characterization of two carotenoid cleavage enzymes from *Arabidopsis* indicates that a carotenoid-derived compound inhibits lateral branching. *J. Biol. Chem.* **279**, 46940-46945
- 33 Booker, J., Auldrige, M., Wills, S., McCarty, D., Klee, H. and Leyser, O. (2004) MAX3/CCD7 is a carotenoid cleavage dioxygenase required for the synthesis of a novel plant signaling molecule. *Curr. Biol.* **14**, 1232-1238
- 34 Auldrige, M. E., Block, A., Vogel, J. T., Dabney-Smith, C., Mila, I., Bouzayen, M., Magallanes-Lundback, M., Dellapenna, D., McCarty, D. R. and Klee, H. J. (2006) Characterization of three members of the *Arabidopsis* carotenoid cleavage dioxygenase family demonstrates the divergent roles of this multifunctional enzyme family. *Plant J.* **45**, 982-993
- 35 Ruch, S., Beyer, P., Ernst, H. and Al-Babili, S. (2005) Retinal Biosynthesis in eubacteria: *in vitro* characterization of a novel carotenoid oxygenase from *Synechocystis* sp. PCC6803. *Mol. Microbiol.* **55**, 1015-1024
- 36 Kloer, D. P., Ruch, S., Al-Babili, S., Beyer, P. and Schulz, G. E. (2005) The structure of a retinal-forming carotenoid oxygenase. *Science* **308**, 267-269
- 37 Barua, A. B. and Olson, J. A. (2000)  $\beta$ -Carotene is Converted Primarily to Retinoids in Rats *in vivo*. *J. Nutr.* **130**, 1996-2001
- 38 Schwede, T., Kopp, J., Guex, N. and Peitsch, M. C. (2003) SWISS-MODEL: an automated protein homology-modeling server. *Nucleic Acid Res.* **31**, 3381-3385
- 39 Krissinel, E. and Henrick, K. (2005) in *Detection of Protein Assemblies in Crystals*. (Berthold, M. R., Glen, R., Diederichs, K., Kohlbacher, O., and Fischer, I. eds.) pp. 163-174, Springer-Verlag Berlin Heidelberg, Germany
- 40 Sanner, M. F., Olson, A. J. and Spehner, J. C. (1996) Reduced surface: an efficient way to compute molecular surfaces. *Biopolymers* **38**, 305-320
- 41 Rippka, R., Deruelles, J., Waterbury, J. B., Herdmann, M. and Stanier, R. T. (1979) Generic assignments, strain histories and properties of pure cultures of cyanobacteria. *J. Gen. Microbiol.* **111**, 1-61

- 42 Ermakova, S. Y., Elanskaya, I. V., Kallies, K. U., Weihe, A., Börner, T. and Shestakov, S. V. (1993) Cloning and sequencing of mutant *psbB* genes of the cyanobacterium *Synechocystis* PCC6803. *Photosynth. Res.* **37**, 139-146
- 43 Robinson, K. R., Lorenzi, L., Ceccarelli, N. and Gaultieri, P. (1998) Retinal identification in *Pelvetia fastigiata*. *Biophys. Res. Commun.* **243**, 776-778
- 44 Chothia, C. and Lesk, A. M. (1986) The relation between the divergence of sequence and structure in proteins. *EMBO J.* **5**, 823-826
- 45 Moise, A. R., von Lintig, J. and Palczewski, K. (2005) Related enzymes solve evolutionarily recurrent problems in the metabolism of carotenoids. *Trends Plant Sci.* **10**, 178-186
- 46 Bouvier, F., Isner, J. C., Dogbo, O. and Camara, B. (2005) Oxidative tailoring of carotenoids: a prospect towards novel functions in plants. *Trends Plant Sci.* **10**, 187-194
- 47 Sabehi, G., Loy, A., Jung, K. H., Partha, R., Spudich, J. L., Isaacson, T., Hirschberg, J., Wagner, M. and Béjà, O. (2005) New insights into metabolic properties of marine bacteria encoding proteorhodopsins. *PLoS Biol.* **3**, e273
- 48 Peck, R. F., Echavarri-Erasun, C., Johnson, E. A., Ng, W. V., Kennedy, S. P., Hood, L., DasSarma, S. and Krebs M. P. (2001) *brp* and *blh* are required for synthesis of the retinal cofactor of bacteriorhodopsin in *Halobacterium salinarum*. *J. Biol. Chem.* **276**, 5739-5744
- 49 Takaichi, S., Mochimaru, M., Maoka, T. and Katoh, H. (2005) Myxol and 4-Ketomyxol 2'-Fucosides, not Rhamnosides, from *Anabaena* sp. PCC 7120 and *Nostoc punctiforme* PCC 73102, and Proposal for the Biosynthetic Pathway of Carotenoids. *Plant Cell Physiol.* **46**, 497-504
- 50 Zorn, H., Langhoff, S., Scheibner, M., Nimtz, M. and Berger, R. G. (2003) A peroxidase from *Lepista irina* cleaves beta,beta-carotene to flavor compounds. *Biol. Chem.* **384**, 1049-1056
- 51 Hihara, Y., Kamei, A., Kanehisa, M., Kaplan, A. and Ikeuchi, M. (2001) DNA microarray analysis of cyanobacterial gene expression during acclimation to high light. *The Plant Cell* **13**, 793-806
- 52 Marin, K., Kanesaki, Y., Los, D. A., Murata, N., Suzuki, I. and Hagemann, M. (2004) Gene expression profiling reflects physiological processes in salt acclimation of *Synechocystis* sp. strain PCC 6803. *Plant Physiol.* **136**, 3290-300
- 53 Al-Babili, S., von Lintig, J., Haubruck, H. and Beyer, P. (1996) A novel, soluble form of phytoene desaturase from *Narcissus pseudonarcissus* chromoplasts is Hsp70-complexed and competent for flavinylation, membrane association and enzymatic activation. *Plant J.* **9**, 601-612
- 54 Xue, L., Gollapalli, D. R., Maiti, P., Jahng, W. J. and Rando, R. R. (2004) A palmitoylation switch mechanism in the regulation of the visual cycle. *Cell* **117**, 761-771
- 55 Enzell, C. R., and Back, S. (1995) in *Carotenoids* (Britton, G., Liaaen-Jensen, S., and Pfander, H., eds) Vol. 1B, p. 264, Birkhäuser Verlag, Basel, Switzerland

## TABLES

**Table 1**

**The  $K_m$  and  $V_{max}$  values of NosACO for different substrates**

Each value represents the average  $\pm$  S.D. of three independent experiments.

| Substrate                            | $K_m$ ( $\mu$ M) | $V_{max}$ (nmol/min) |
|--------------------------------------|------------------|----------------------|
| $\beta$ -8'-apo-carotenal            | 16.3 $\pm$ 1.6   | 1.0 $\pm$ 0.3        |
| $\beta$ -10'-apo-carotenal           | 17.2 $\pm$ 1.8   | 0.3 $\pm$ 0.1        |
| (3R)-3-OH- $\beta$ -8'-apo-carotenal | 2.1 $\pm$ 0.3    | 0.1 $\pm$ 0.04       |
| $\beta$ -8'-apo-carotenol            | 24.5 $\pm$ 3.1   | 3.3 $\pm$ 1.7        |

## FIGURE LEGENDS

**Figure 1 HPLC analyses of the *in vitro* assay products obtained from  $\beta$ -apo-8'-carotenal (A),  $\beta$ -apo-10'-carotenal (B) and (3R)-3-OH- $\beta$ -apo-8'-carotenal (C) and the corresponding UV/Vis spectra (I-III)**

After 2.5 h incubation with purified NosACO (ACO), a striking cleavage activity was observed, indicated by color changes compared to the controls (con). The reactions led to the formation of the products apo-8',15'-apo-carotene-dial (I) and retinal (II) from  $\beta$ -apo-8'-carotenal (A), retinal (II) from  $\beta$ -apo-10'-carotenal (B) and (3R)-3-OH-retinal (III) and apo-8',15'-apo-carotene-dial (I) from (3R)-3-OH- $\beta$ -apo-8'-carotenal (C). The structure of the products is given above the corresponding UV/Vis spectra, see also Fig. 2 and Fig. 3.

**Figure 2 GC-MS analyses of the *in vitro* assay products**

The products obtained from *in vitro* assays (Fig. 1) were subjected to GC-MS analyses. The EI mass spectrum of product I was identical to that obtained with synthetic apo-8',15'-apo-carotene-dial ( $C_{10}O_2H_{11}$ ) and showed the expected molecular mass of  $m/z$  164. The EI mass spectrum of product II showed identity with the reference spectrum of retinal and the expected molecular ion of  $m/z$  284. The EI mass spectrum of product III showed identity with the reference spectrum and the expected molecular ion of  $m/z$  300 as well as the typical fragment of 162  $m/z$ , corresponding to a mass of 300 minus 138, indicative for the loss of the 3-OH- $\beta$ -ionone ring as described for zeaxanthin [55].

### Figure 3 Structure of applied substrates and determined products (I-III)

The degree of cleavage was estimated by the ratio of cleavage product compared to the substrate. ++ cleavage; + low cleavage; n.d. not detected. The substrates  $\beta$ -apo-8'-carotenal ( $C_{30}$ ), its corresponding alcohol and  $\beta$ -apo-10'-carotenal ( $C_{27}$ ) were cleaved into retinal ( $C_{20}$ , II). (3R)-3-OH- $\beta$ -apo-8'-carotenal, its corresponding alcohol and (3R)-3-OH- $\beta$ -apo-12'-carotenal ( $C_{25}$ ) were converted to (3R)-3-OH-retinal (III). Apo-8',15'-apo-carotene-dial ( $C_{10}$ , I) was produced from the cleavage of the  $\beta$ -apo-8'-carotenoids ( $C_{30}$ ) as the second product. Substrates were cleaved at the C15-C15' double bond, as indicated. With exception of apo-12'-lycopenals, the enzyme converted all applied apo-lycopenals into the corresponding  $C_{20}$ -compound acycloretnal (not shown). The incubation with  $\beta$ -apo-4'-carotenal and  $\beta$ -apo-12'-carotenal did not lead to detectable products.

### Figure 4 Model of NosACO based on homology to SynACO

A: Ribbon representation of NosACO.  $\beta$ -strands and  $\alpha$ -helices are drawn in orange and green, respectively. The eight residues forming the large hydrophobic patch at the top of the enzyme are shown in stick representation and labeled. The axis of the  $\beta$ -propeller runs vertically. B: Surface representation showing the solvent-accessible surface in grey. The entrance to the substrate binding tunnel is drawn in blue and the hydrophobic patch of 889 Å<sup>2</sup> in yellow. C: Geometry of the substrate binding tunnel. Surface representation of NosACO rotated by 90° along the propeller axis and cut through the middle of the enzyme. The substrate binding tunnel runs horizontally and is shaded in blue. The position of the catalytic iron is indicated in red. In order for cleavage to occur, the substrate must enter the tunnel far enough to bring the scissile double bond in close proximity to the catalytic iron. A constriction in the tunnel, marked by arrows, prevents entry of bulky substrates. D: Close-up view of the constriction together with a  $\beta$ -ionone ring for size comparison. The constriction is too small to allow substrates carrying  $\beta$ -ionone rings on both termini such as  $\beta$ -carotene to enter the tunnel.

### Figure 5 Western blot analysis of the reconstitution assay

Total reconstitution assay containing soluble and liposome-bound NosACO (1), isolated and washed liposomes (2), the corresponding supernatant containing unreconstituted enzyme (3), liposomes after treatment with 0.2 M KCl (4) and the corresponding supernatant (5). NosACO was detected using polyclonal anti-Syn-ACO-antibodies.

### Figure 6 Localization of SynACO in a *Synechocystis* *SynDiox2* knock-out strain

A: Coomassie stained SDS-gel of membrane (1) and cytoplasmic fraction proteins (2). B: The corresponding Western blot analysis. The localization was performed using 25 µg protein of each fraction.

# FIGURES

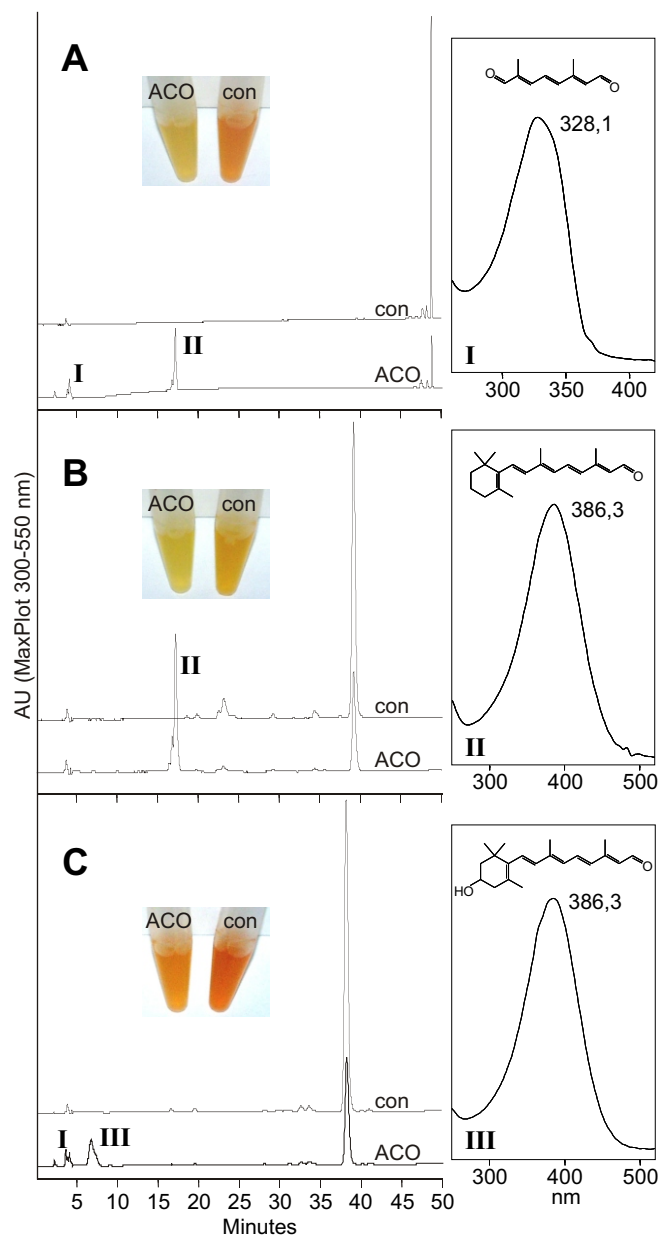


Fig. 1

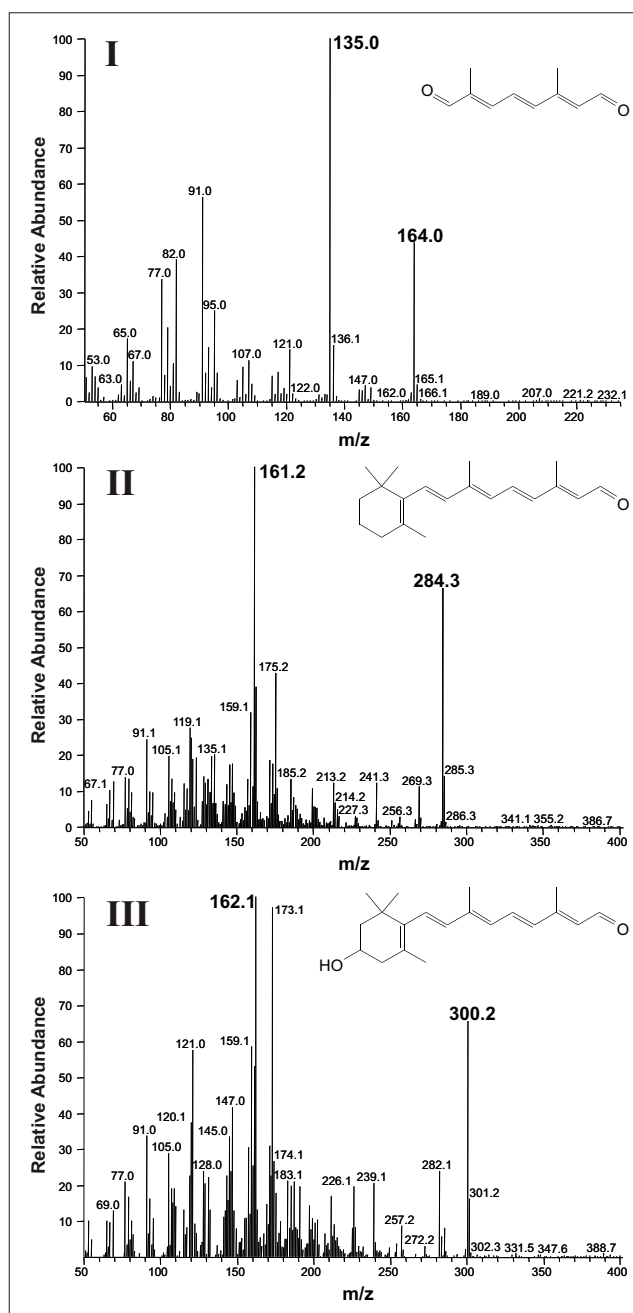


Fig. 2

|  | Substrate                               | Cleavage |  |
|--|---|----------|--|
| chain length   | $\beta$ -apo-4'-carotenal ( $C_{35}$ )  | n.d.     |  |
|  | $\beta$ -apo-8'-carotenal ( $C_{30}$ )  | ++       |  |
|  | $\beta$ -apo-10'-carotenal ( $C_{27}$ ) | ++       |  |
|  | $\beta$ -apo-12'-carotenal ( $C_{25}$ ) | n.d.     |  |
| substitution<br>of the $\beta$ -ring   | (3R)-3-OH- $\beta$ -apo-8'-carotenal    | ++       |  |
|  | (3R)-3-OH- $\beta$ -apo-12'-carotenal   | +        |  |
|  | apo-8'-lycopenal                        | +        |  |
|  | apo-10'-lycopenal                       | ++       |  |
|  | apo-12'-lycopenal                       | n.d.     |  |
| alcohols   | $\beta$ -apo-8'-carotenol               | ++       |  |
|  | (3R)-3-OH- $\beta$ -apo-8'-carotenol    | ++       |  |
|  | apo-8'-lycopenol                        | +        |  |
| <div><div><b>I</b><br/></div><div><b>II</b><br/></div><div><b>III</b><br/></div></div> |   |          |  |

Fig. 3



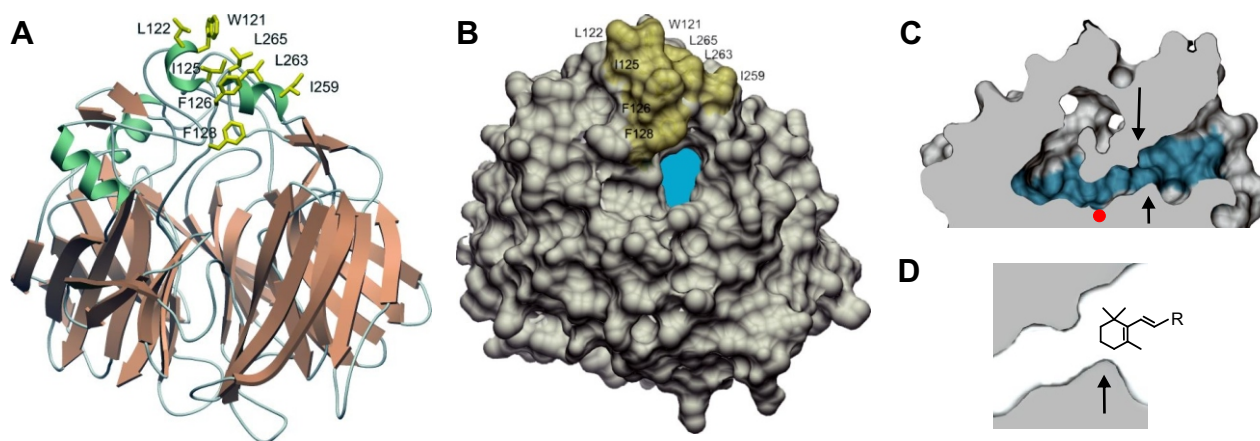


Fig. 4

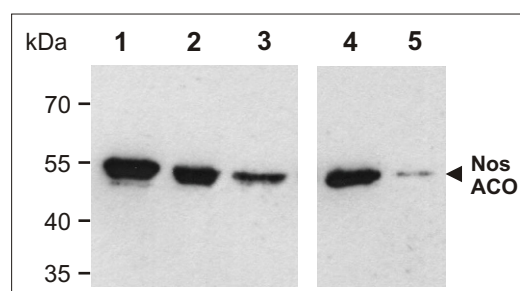


Fig. 5

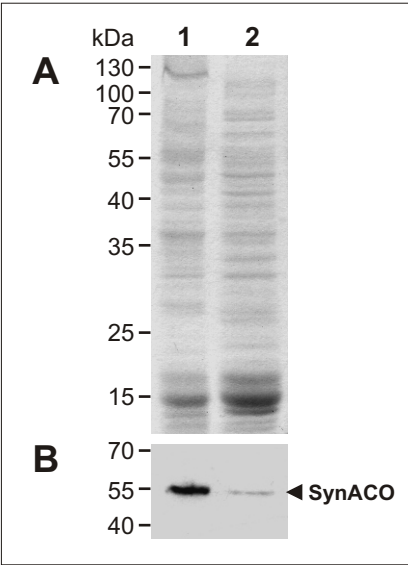


Fig. 6